Overexpression of *PtaHDG11* enhances drought tolerance and suppresses trichome formation in *Populus tremula* × *Populus alba*

Alexander Fendel, Matthias Fladung, Tobias Bruegmann*

Thünen Institute of Forest Genetics, Sieker Landstrasse 2, D-22927 Grosshansdorf, Germany

*Corresponding author: tobias.bruegmann@thuenen.de, tobias.bruegmann@tobiology.de

Keywords: drought stress, forest trees, gene overexpression, poplar, transgenic trees, trichomes

ORCIDs:

AF: https://orcid.org/0000-0001-6606-657X

MF: https://orcid.org/0000-0001-9301-8581

TB: https://orcid.org/0000-0001-9823-5630

Main Conclusion

PtaHDG11 overexpression enhanced drought tolerance in a transgenic poplar hybrid by attenuating the stress response, characterized by increased leaf RWC, increased expression of antioxidant genes, and reduced oxidative damage.

Abstract

The consequences of climate change threaten the long-term sustainability of forests in Central Europe. In particular, extended drought periods are increasingly impacting the growth and survival of forest trees, underscoring the need for innovative approaches to adapt trees to drought. A deeper understanding of the functions of genes involved in drought tolerance can contribute to the development of effective strategies to address drought-related challenges. The homeobox-leucine zipper protein HDG11 has been identified as a promising target for enhancing drought stress tolerance in plants; however, the functional role of the native *HDG11* gene in tree species remains uncharacterized. To address this, we identified the homolog of the *AtHDG11* gene in the poplar hybrid *Populus tremula* × *Populus alba* and subsequently transformed the *PtaHDG11* gene into the poplar hybrid clone INRA 717-1B4 for constitutive overexpression. Drought stress experiments revealed significantly enhanced drought stress tolerance in *PtaHDG11*-overexpressing poplars compared to the wildtype.

This improved tolerance was characterized by reduced proline and malondialdehyde accumulation, increased relative leaf water content, decreased leaf shedding rates, and elevated expression of antioxidant-related genes, including *SOD* and *CAT*. Increased tolerance resulted in significantly increased dry biomass after the recovery phase. Notably, the *PtaHDG11*-overexpressing poplars presented a glabrous phenotype and lacked trichomes. Our study demonstrated the potential of *PtaHDG11* to increase drought stress tolerance in trees by enhancing ROS detoxification and improving leaf water retention. These findings suggest that *HDG11* is a promising candidate for improving drought resilience in trees, with implications for sustainable forest management and breeding programs.

Introduction

The genus *Populus* comprises economically important tree species that are distributed in temperate regions worldwide. Owing to their rapid growth, modest environmental requirements, wood quality, and ease of propagation, poplars are cultivated in short-rotation coppices. Poplars are often utilized in various industrial applications, such as the production of raw materials for the timber industry and paper manufacturing (Komán et al. 2023), as well as the production of biofuels and biorefineries, contributing to renewable energy sources (An et al. 2021). Furthermore, the use of poplar for genetic functional studies yields important information for refined forest tree breeding and the potential direct use of genetically modified poplar, where permitted. In this context, investigating the mechanisms underlying drought tolerance in poplars is essential, as this knowledge can be applied to improve the resilience of forest ecosystems, which are under increasing threat due to climate change. In particular, over the past eight years, European forests have been increasingly vulnerable to weather extremes, with notable increases in the frequency and intensity of summer droughts (Schuldt et al. 2020; Bastos et al. 2021). Such drought periods are predicted to become even more frequent and severe in the coming years, with climate models forecasting a significant increase in drought intensity and duration across European forests (Knutzen et al. 2025). Therefore, the breeding of drought-tolerant trees, including poplars, has become a challenging demand (Zhao et al. 2023).

Drought stress tolerance refers to a plant's ability to maintain the potential for optimal physiological functions, growth, and survival under water-limited conditions (Fang and Xiong 2015). This encompasses both the plant's capacity to mitigate the negative impacts of drought through various morphological, physiological, molecular physiological, and cellular adjustments during stress and its subsequent ability to recover efficiently and resume productive growth (fitness) once water availability is restored (Polle et al. 2018). Crucially, the long-term productivity and reproductive success of a plant following a drought event are key indicators of true tolerance, extending beyond mere survival during the stress period.

Drought stress leads to the formation of cellular reactive oxygen species (ROS), which are generated through the disruption of cellular homeostasis, such as the inhibition of photosynthetic electron transport. The accumulation of ROS can also trigger a range of signaling pathways, including those involved in the stress response and programmed cell death (Apel and Hirt 2004). The detrimental effects of ROS can be mitigated by the action of antioxidative enzymes, such as superoxide dismutase (SOD) or catalase (CAT). SOD and CAT are essential components of the plant antioxidant defense system and play crucial roles in detoxifying ROS. SOD acts as the primary defense mechanism against ROS, catalyzing the conversion of superoxide anions to hydrogen peroxide and molecular oxygen. Additionally, CAT further detoxifies hydrogen peroxide by converting it into water and oxygen, thereby protecting plant cells from oxidative damage (Leung 2018). Molecular physiological responses to drought include the accumulation of proline, an amino acid with osmoprotectant properties, which has been observed in various plant species, including several hybrid poplar genotypes and *Populus euphratica* (Chen et al. 2003; Barchet et al. 2014).

71 The key players in those stress adaptive mechanisms are transcription factors (TFs), which can regulate the
72 expression of genes involved in stress responses (Joshi et al. 2016; Manna et al. 2021). The homeodomain-leucine
73 zipper (HD-ZIP) protein family plays a central role in plant development, including processes such as
74 organogenesis and leaf development (Roodbarkelari and Groot 2017; Tu et al. 2022). For example, HD-ZIP IV
75 members bind HD-ZIP-cis elements that are frequently present in the promoters of expansin, extensin, or
76 xyloglucan-endo-transglycosylase/hydrolase (*XTH*) genes, thereby regulating cell-wall extensibility (Xu et al.
77 2014). HD-ZIP TFs are also involved in stress responses. In particular, the *HDG11* gene, which belongs to HD-ZIP
78 subfamily IV, has emerged as a promising target for enhancing drought tolerance. At present, functional studies
79 of *HDG11* have focused almost exclusively on *AtHDG11* from the model plant species *Arabidopsis thaliana.* The
80 increased expression of *AtHDG11* in *A. thaliana* and *Nicotiana tabacum* significantly enhances drought tolerance
81 by reducing leaf stomatal density, increasing root system development, increasing proline and abscisic acid
82 accumulation, and, in general, activating genes involved in stress response pathways (Yu et al. 2008). Similarly,
83 the overexpression of *AtHDG11* in tall fescue (*Festuca arundinacea*) improved drought and salt stress tolerance
84 via increased ROS-scavenging ability (Cao et al. 2009). Similar results have been reported for sweet potato
85 (*Ipomoea batatas*; Ruan et al. 2012), rice (*Oryza sativa*; Yu et al. 2013), Chinese kale (*Brassica oleracea*; Zhu et
86 al. 2016), and upland cotton (*Gossypium hirsutum; Yu et al. 2016*). In addition, Yu et al. (2016) reported that
87 *AtHDG11* overexpression in Chinese white poplar (*Populus* × *tomentosa*) improved drought and salt stress
88 tolerance, resulting in a more developed root system, reduced leaf stomatal density, and increased stomatal and
89 leaf epidermis cell size.

90 While the functions of the *AtHDG11* gene have been extensively studied in various organisms, the native *HDG11*
91 potential in tree species remains unexplored. This study aims to address this knowledge gap by examining the
92 role of *PtaHDG11* in the drought tolerance of the poplar hybrid *Populus tremula* × *Populus alba*. Notably, despite
93 drought stress tolerance being a complex trait involving multiple genes, the overexpression of a single gene copy
94 from the *P. alba* allele (gene number PtXaAlbH.15G026700) in the poplar hybrid clone significantly improved
95 drought stress tolerance under controlled conditions, making it a promising target for further research and
96 contributing to the development of forest stands with increased drought resilience. Additionally, we also
97 revealed that this gene is involved in trichome formation.

98 Materials and Methods

99 Identification and bioinformatic analysis of candidate gene

100 To identify the *PtaHDG11* gene in *P. tremula* × *P. alba*, we utilized the protein sequence of *At*HDG11 from
101 *A. thaliana* (AT1G73360) as the query sequence. A BLAST search was performed against the genomes of
102 *P. tremula* × *P. alba* HAP1 v5.1 and HAP2 v5.1, which were accessed through the Phytozome database (Goodstein
103 et al. 2012). The protein sequences of *A. thaliana*, both *P. tremula* × *P. alba* alleles, and *Populus trichocarpa* were

104 retrieved from the Phytozome database and aligned using the Multiple Sequence Alignment by CLUSTALW tool
105 (https://www.genome.jp/tools-bin/clustalw) and subsequently visually adjusted via Jalview (Waterhouse et al.
106 2009). Protein domains were identified via the SMART web resource (Letunic et al. 2021). A phylogenetic tree
107 was constructed via the Maximum Likelihood Method (bootstrap with 1000 replications) via the MEGA11
108 program (Tamura et al. 2021). The tree included all genes of the *A. thaliana* HD-ZIP IV class (as described in
109 Nakamura et al. (2006)) and the poplars' *AtHDG11* homologous genes.

110 **Plant materials and *in vitro* growth conditions**

111 The study was conducted with the poplar hybrid clone INRA 717-1B4 (*P. tremula* × *P. alba*; Leple et al. (1992)).
112 The maintenance and propagation of the wild type (WT) and the subsequently produced transformation lines
113 were performed *in vitro* on solid McCown Woody Plant Medium supplemented with vitamins (WPM; supplied by
114 Duchefa, Haarlem, The Netherlands), 2% (w/v) sucrose, and 0.6% (w/v) agar at a pH of 5.8. The *in vitro* cultures
115 were maintained in Magenta vessels under controlled conditions at 23 °C with approximately 50% relative
116 humidity (RH). Continuous 24-hour light was provided by LED lamps, which delivered a photosynthetic photon
117 flux density of approximately 170 µmol m^{-2} s^{-1}.

118 **Transformation vector and candidate gene transformation**

119 The binary vector for the constitutive overexpression of *PtaHDG11* was obtained from DNA Cloning Service
120 (Hamburg, Germany; Online Resource 1). The T-DNA region of the vector contained the 35S::*nptIIo* selection
121 marker gene, as well as the coding sequence (CDS) of *PtaHDG11*, which was driven by an *AtUBQ10* promoter.
122 The recombinant plasmid was introduced into the *Agrobacterium tumefaciens* strain GV3101-pMP90RK and
123 subsequently transformed into the poplar WT via a modified leaf disc transformation method (Bruegmann et al.
124 2019). Successfully transformed poplars were regenerated on WPM supplemented with cefotaxime (500 mg/L)
125 to eliminate residual *A. tumefaciens*, kanamycin (50 mg/L) for the selection of successful transformants, and
126 Pluronic F-68 (100 mg/L) and thidiazuron (0.0022 mg/L) to promote efficient regeneration of the plantlets.

127 **Verification of genetic transformation in putative poplar lines**

128 After transformation, 9 regenerants were obtained, of which only three lines survived the antibiotic selection
129 process. Genomic DNA was isolated from the regenerated transgenic poplar lines HDG11-1, HDG11-2, and
130 HDG11-3 via the method described by Bruegmann et al. (2022). The putative transgenic lines were identified via
131 standard PCRs targeting the *nptIIo* and *PtaHDG11* genes via primers located on the promoter and terminator of
132 the cassettes. Southern blot analysis was subsequently performed to determine the number of integrated T-DNA
133 sequences in the putative overexpression lines (Fladung and Ahuja 1995). Additionally, PCRs targeting the
134 streptomycin/spectinomycin resistance gene of the transformation plasmid backbone were performed to
135 exclude the presence of residual *A. tumefaciens* bacteria within the putative transformation lines, interfering

with the results of the transformation verification analyses. The T-DNA integration locus was identified via Thermal Asymmetric Interlaced PCR (TAIL-PCR), as described by Liu et al. (1995) and Fladung and Polak (2012). All the PCR primers used are listed in Online Resource 2. The obtained Sanger sequences of the integration loci, provided by StarSeq (Mainz, Germany), were then compared to the two *P. tremula* × *P. alba* haplotypes (HAP1 and HAP2) using BLAST analysis via the Phytozome database.

Drought stress experimental setup

A three-week greenhouse experiment was conducted from November 22 to December 13, 2023. Rooted head cuttings from the HDG11-2 transformation line and the WT control were transferred from *in vitro* culture to sieved tree nursery soil (Profisubstrat Ton+; Gramoflor, Vechta, Germany). Fourteen equally growing individual plants of both lines were potted to a final pot size of 3 L. The plants were cultivated under controlled conditions with a consistent 16/8 h light/dark regime, 22 °C, and 60% RH. The pots were randomly placed on a greenhouse bench in a 22 × 4 placement, with additional WT plants around the experiment to buffer side effects from environmental fluctuations. When the plants reached a height of approximately 30 cm, drought stress was applied to half of the plants, while the other half received regular irrigation (130 mL) using an automatic drip irrigation system (Rain Bird Corporation; Azusa, CA, USA), which served as the control group for each line. Pot saucers were placed upside down underneath each experimental plant for runoff of excess water and to avoid water accumulation in the root zone. At the beginning of the experiment, all the plants were equally irrigated with 1 L for complete soil saturation. The experimental plants were phenotyped once per week, and sampling was carried out at four time points (no stress = start of the experiment, moderate stress = 7 days of drought stress, severe stress = 14 days of drought stress, and recovery = 7 days of rewatering) to target specific stages of the plants' drought stress response. The soil moisture levels of each pot were monitored on each sampling day via a micro station data logger and soil moisture sensors (HOBO U21 USB and HOBO EC5 Soil Moisture Smart Sensor; Onset Computer Corp., Bourne, MA, USA).

As a second approach, a three-week climate chamber experiment was conducted from January 23 to February 13, 2025, to validate the findings from the earlier greenhouse experiment. Rooted head cuttings from the transformation line HDG11-2 and WT were transferred from *in vitro* culture to soil as previously described. The transferred plants were then acclimatized to the climate chamber conditions (Weiss Technik, Lindenstruth, Germany) in a sealed container with a 16/8 h light/dark cycle with 16 µmol m^{-2} s^{-1} photosynthetic photon flux density (PPFD), 22/17 °C temperature, and 70% RH, with a gradual opening of the lid over a 10-day period. The plantlets were subsequently transferred into 1 L cultivation pots until they reached a height of approximately 30 cm. All plants were then randomly arranged in the climate chamber with unchanged adjustments and approx. 35 µmol m^{-2} s^{-1} PPFD. Here, 14 individuals per line were subjected to drought conditions without irrigation, whereas six individuals per line were manually irrigated daily with 100 mL of water per day. The experimental plants were phenotyped once per week, and sampling was carried out at three time points (no stress = start of

170 the experiment, severe stress = 7 days of drought stress, and recovery = 14 days of rewatering). The soil moisture
171 levels of each pot were monitored during the severe stress phase as described above.

172 **Measurement of morphological, physiological, and molecular indicators**

173 *Relative water content*

174 To measure the relative water content (RWC), the 3rd fully expanded leaf from each plant was excised in both
175 experiments, specifically under severe stress and rewatering conditions. The cut leaves were immediately
176 weighed to obtain the fresh weight (FW). The leaves were subsequently submerged in a container filled with
177 distilled water to achieve full turgidity. After a period of 24 h, the leaves were removed from the water, excess
178 water was gently blotted off, and the turgid weight (TW) was recorded. The leaves were subsequently dried in
179 an oven at 80 °C for 48 h and then weighed again to obtain the dry weight (DW). The RWC was calculated as RWC
180 = (FW [g] - DW [g]) / (TW [g] - DW [g]) × 100 [%].

181 *Proline quantification*

182 Proline was measured from the 4th fully expanded leaf, according to Bates et al. (1973), and adapted to a
183 microplate-based protocol (Abrahám et al. 2010). In brief, 50 mg of leaf material was homogenized in a bead
184 ruptor under steady cooling. To extract disturbing proteins, each sample was mixed with 1 mL of 5-sulfosalicylic
185 acid and centrifuged at 12,000 × g for 10 min. Two hundred microliters of the supernatant were mixed with
186 ninhydrin, acetic acid, and phosphoric acid and incubated at 96 °C. The reaction was stopped on ice, and each
187 sample was supplemented with 1 mL of toluene to extract the proline-ninhydrin mixture. The determination of
188 proline content was conducted by measuring the absorbance of the toluene proline mixture at 520 nm in a 96-
189 well plate via a microplate reader (SPECTROstar Nano; BMG LABTECH, Ortenberg, Germany). Proline
190 accumulation was determined via the standard curve method.

191 *Malondialdehyde quantification*

192 Lipid peroxidation was determined by quantification of malondialdehyde (MDA) according to Hodges et al.
193 (1999). One hundred milligrams of the 4th fully expanded leaf was homogenized under steady cooling and mixed
194 with 1.5 mL of 0.1% trichloroacetic acid to precipitate proteins. Five hundred microliters were then mixed with
195 reaction solution 1 (comprising 0.01% 2,6-di-ter-butyl-4-methylphenole and 20% trichloroacetic acid) and
196 another 500 µL with reaction solution 2 (comprising reaction solution 1 with an additional 0.65% 2-thiobarbituric
197 acid) and subsequently incubated at 96 °C for 30 min. The reaction was stopped on ice and centrifuged at 8,000
198 × g and 4 °C for 10 min. MDA was determined via photometry at 440, 532, and 600 nm using the microplate
199 reader. The MDA levels were calculated based on the formulas Hodges et al. (1999) and Landi (2017).

Total shoot biomass

To determine the total shoot biomass, all shoots of the plants from the growth chamber experiment were isolated from the below-ground biomass, and the fresh weights of all the leaves and stems per sample were weighed. Afterward, the leaves were oven dried at 80 °C for 48 h, and the stems were oven dried at 105 °C for 24 h, after which the shoot dry weight was measured.

Height and stem diameter

The height of each plant was measured using a standard folding rule from the base of the stem to the tip of the shoot. Additionally, the stem diameter was measured with a vernier caliper at a height of 10 cm above the base of the shoot.

Number of leaves

On each sampling day, the fully expanded leaves of each individual plant were counted. A fully expanded leaf was defined as a leaf measuring ≥ 2.5 cm in diameter (typically the 2nd or 3rd leaf from the apex). After each sampling day, the shoot tips above the first fully expanded leaf were labeled to accurately determine the number of newly formed leaves.

Stomatal conductance

Stomatal conductance was measured via an SC-1 leaf porometer (METER Group, Pullman, WA, USA). Measurements were conducted on the 3rd fully expanded leaf of each plant.

Chlorophyll quantification

The chlorophyll content in the leaves was quantified via DUALEX (Force-A, Orsay, France) on the 3rd fully expanded leaf of each plant.

Stomatal density and trichome observation

Trichome removal and stomatal counting were performed according to the protocol described by Wodtke et al. (2025). For each line, three leaves from *in vitro*-grown plantlets were selected for analysis. The stomata were visualized under a light microscope (Axioscope 5; ZEISS, Oberkochen, Germany) and subsequently counted using the ImageJ 1.54p software (Schneider et al. 2012) to determine the stomatal density (number of stomata per mm^2). Trichome observation was carried out on *in vitro*-grown plantlets of the three lines using a light microscope (Stemi 2000-C; ZEISS, Oberkochen, Germany).

227 **Gene expression analyses**

228 Quantitative real-time PCR (RT-qPCR) was performed to analyze the expression levels of the selected genes
229 *HDG11*, *GLABRA 2* (*GL2*), and *STOMATAL DENSITY AND DISTRIBUTION 1* (*SDD1*), as well as *A. thaliana* homologs
230 of *SUPEROXIDE DISMUTASE 2* (*SOD2-like*), *CATALASE 2* (*CAT2-like*), and *XYLOGLUCAN:XYLOGLUCOSYL*
231 *TRANSFERASE 32* (*XTH32-like*), identified through BLAST analysis and designated as '-like' genes, in the WT and
232 the transgenic line. Total RNA was isolated from the leaf tissue of three biological replicates per line and
233 harvested during the severe stress in the greenhouse experiment. The RNA isolation was performed according
234 to Bruegmann et al. (2024), using the innuPREP Plant RNA Kit (IST Innuscreen; Berlin, Germany). cDNA synthesis
235 and RT-qRT-PCR were carried out via the GoTaq 2-Step RT-qPCR System (Promega Corp.; Madison, WI, USA)
236 following the manufacturer's instructions. The C1000 Touch Thermal Cycler (Bio-Rad Laboratories Inc.; Hercules,
237 CA, USA) was programmed with the following settings: initial denaturation at 95 °C for 2 min, followed by 40
238 cycles of 95 °C for 15 s and 58 °C for 1 min. The specific amplification of each target gene was analyzed using a
239 melting curve (95 °C for 15 s, 59 °C for 1 min). The relative expression of each target gene was calculated
240 according to the $2^{-\Delta\Delta Ct}$ method (Livak and Schmittgen 2001). Measurements were normalized to the poplar
241 *UBIQUITIN* (*PtaUBQ*) housekeeping gene (Regier and Frey 2010).

242 **Statistical analyses**

243 All analyses were performed in R version 4.4.2 (R Core Team 2024) and RStudio version 2024.12.0.467 (Posit
244 team 2024). Repeated-measure traits were modeled using linear mixed-effects models (lme4, lmerTest) with
245 line, treatment, and sampling day as fixed effects and plant individual as a random intercept. For each trait,
246 model fit and residual diagnostics (Shapiro–Wilk, Levene's test, DHARMa) were evaluated for both raw and log+1-
247 transformed data. The transformation yielding residuals closest to normality and homoscedasticity was selected
248 for final modeling. Fixed effects were assessed by Type III ANOVA, with pairwise contrasts of estimated marginal
249 means adjusted by Holm's method. Traits measured only once were analyzed using univariate tests (Student's t-
250 test or Welch's t-test), depending on homogeneity of variances. Outliers were removed within each subline and
251 treatment group for each trait using the interquartile range (IQR) method. Statistical significance was set at α =
252 0.05. Spearman's rank correlation coefficient (ρ) was used to assess monotonic relationships between
253 physiological, morphological, and biochemical traits during the severe stress phase.

254

255 ## Results

256 The BLAST search of the *At*HDG11 protein sequence identified two paralogous genes in both alleles of
257 *P. tremula* × *P. alba* (Fig. 1a). The analysis revealed that the gene *PtXaAlbH.15G026700* from the hybrid's *P. alba*
258 allele exhibited the highest protein similarity (70.9%). The Maximum Likelihood phylogenetic analysis of the HD-
259 ZIP IV subfamily revealed that the *AtHDG11*/*HDG12* cluster and the corresponding *Populus* cluster diverged from
260 a common ancestor with high statistical support (Bootstrap 99), confirming the orthologous relationship of the
261 entire *Populus* group consisting of both *P. tremula* × *P. alba* alleles and *P. trichocarpa* (Fig. 1b).
262 *PtXaAlbH.15G026700,* the closest homolog, was selected as the candidate gene, referred to as *PtaHDG11*.

263 A comparative analysis of the protein sequences of *HDG11* genes was conducted via multiple sequence
264 alignment, incorporating the HDG11 protein sequences of *P. tremula* × *P. alba*, *A. thaliana*, and *P. trichocarpa*
265 (Fig. 1c). The two *P. tremula* × *P. alba* alleles presented only 3 amino acid (AA) differences within the 707 AA
266 protein, indicating a high degree of similarity between them. The comparison between the species revealed
267 several AA differences between the groups. Specifically, 68% of the AA sequence of the poplar hybrid was
268 identical to that of *A. thaliana*, with 256 AA differences observed between the two species. The alignments of
269 the *P. tremula* × *P. alba* alleles and *P. trichocarpa* alleles were more similar, with differences in 8 AAs between
270 *P. trichocarpa* and the *P. tremula* allele and in 9 AAs compared with the *P. alba* allele. Differences occurred
271 mainly at the N- and C-termini or outside of conserved protein domains. Notably, the protein sequences of the
272 two poplar species presented nearly perfect similarity within the conserved protein domains of HOX and START,
273 which classify the HD-ZIP IV class, with only two exceptions in the START domain at AA positions 264 and 320.
274 Interestingly, the AA differences in the HOX domain occurred mostly in the first half of the domain, whereas the
275 second half, which includes the helix III region (Nakamura et al. 2006), was identical across all species, except for
276 an AA change from leucine in *A. thaliana* to methionine in poplars.

(a)

	Gene				Protein	
Organism	**Gene identifier**	**Chr.**	**CDS length (bp)**	**Exons**	**Length (AA)**	**Similarity to *A. thaliana* (%)**
P. tremula × P. alba	*PtXaTreH.12G026600*	12	2139	10	713	69.8
P. tremula × P. alba	*PtXaAlbH.12G027100*	12	2136	10	712	70.0
P. tremula × P. alba	*PtXaTreH.15G025800*	15	2124	10	708	70.7
P. tremula × P. alba	*PtXaAlbH.15G026700*	15	2124	10	708	70.9
P. trichocarpa	*Potri.012G038500*	12	2136	10	712	70.2
P. trichocarpa	*Potri.015G034100*	15	2124	10	708	71.0
A. thaliana	*AT1G73360*	1	2169	10	722	

(b)

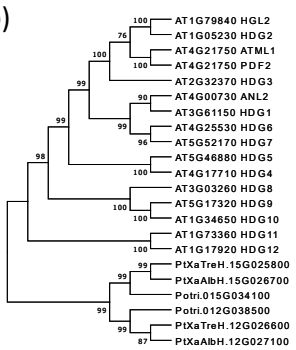

(c)

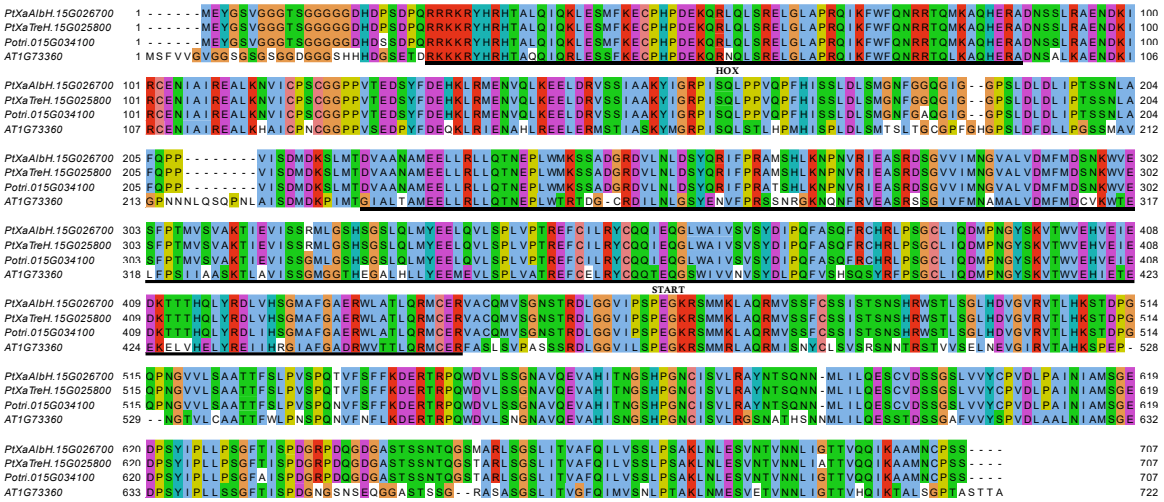

Fig. 1 Identification of the candidate gene *PtaHDG11*. (a) Overview of genetic and protein-related data of *AtHDG11* homologs identified via BLAST analysis, including protein similarity. (b) Phylogenetic tree with all *A. thaliana* HD-ZIP IV genes and all identified poplar homologs of *AtHDG11.* (c) Multiple protein sequence alignment (CLUSTALW) of the *HDG11* gene from both *P. tremula* × *P. alba* alleles (*PtXaAlbH.15G026700*, *PtXaTreH.15G025800*), *P. trichocarpa* (*Potri.015G034100*), and *A. thaliana* (*AT1G73360*), visualized via Jalview. The two HD-ZIP IV protein domains HOX and START are underlined in black

Agrobacterium-mediated transformation and subsequent *in vitro* regeneration yielded three individual lines, which were confirmed to be transgenic by PCR analysis of the *nptIIo* marker gene and the transgenic *PtaHDG11*. However, subsequent Southern blot analysis revealed clear triple T-DNA integration only in HDG11-2. In contrast, HDG11-1 and HDG11-3 could not be demonstrated to carry stable T-DNA insertions. Therefore, only line HDG11-2 was considered for all the following experiments. Finally, the T-DNA integration sites in HDG11-2 were detected via TAIL-PCR. All detected T-DNA integration events occurred exclusively in noncoding regions of the genome.

292 *Greenhouse stress experiment*

293 The WT and HDG11-2 lines were subsequently used for a greenhouse drought stress experiment to assess their
294 performance under water-limited conditions. The greenhouse drought stress experiment was conducted for 21
295 days, with a sampling day every 7th day. The measurement of soil moisture revealed no significant differences in
296 VWC between the two lines within a treatment group on any sampling day (Online Resource 3).

297 Under moderate stress, both lines began to exhibit signs of stress, but significant growth cessation was not
298 observed until the severe stress phase. In the control groups, a steady increase in plant height of approximately
299 30 cm was observed throughout the experiment. In contrast, the stress treatments led to a significant reduction
300 in plant height compared with that of the corresponding control groups on the severe stress and recovery
301 sampling days, with the WT showing the greatest difference (HDG11-2 $p < 0.01$; WT $p < 0.001$). Although no
302 significant differences in plant height or stem diameter were found between the tested lines within a treatment
303 on a given sampling day, the stress treatments resulted in a consistent pattern of growth reduction in both lines.
304 Under recovery conditions, HDG11-2 presented a mean increase in height of approximately 4 cm greater than
305 that of the WT (Fig. 2a). The analysis of stem diameter revealed significant differences between the same line
306 under different treatments. Under severe stress, compared with the control plants, the WT and HDG11-2 plants
307 presented reduced stem diameters ($p < 0.05$, Fig. 2b). This effect was also consistent during recovery (HDG11-2
308 $p < 0.01$; WT $p < 0.05$).

309 Similar to tree height and stem diameter, the number of fully expanded leaves increased steadily in the control
310 groups of both lines (Fig. 2c). Compared with the control plants, the stressed plants presented significant
311 differences in leaf number under severe stress ($p < 0.001$). During recovery, HDG11-2 presented a significantly
312 greater leaf number than did the WT (19 vs. 12; $p < 0.01$).

313 Additionally, we counted the number of new fully expanded leaves, which represents the potential for leaf
314 growth under drought stress conditions (Fig. 2d). Under severe stress, both the WT and HDG11-2 lines presented
315 severe reductions in new leaf formation compared with their respective controls ($p < 0.001$). During the 7-day
316 recovery period, three out of seven stress-treated WT trees failed to produce new leaves. In contrast, HDG11-2
317 recovered its ability to form new leaves in all individuals, reaching nearly the levels observed during moderate
318 stress. Here, HDG11-2 outgrew the WT by 3 new fully expanded leaves ($p < 0.001$). Interestingly, the WT control
319 plants presented a reduced number of new fully expanded leaves over the course of the experiment, resulting in
320 a significant difference from the control plants of HDG11-2 after 21 days (recovery; $p < 0.05$) and also a significant
321 difference from their own new fully expanded leaves during the moderate stress timepoint after 7 days ($p < 0.01$).

322 The stomatal conductance was measured on each sampling day on the 3rd fully expanded leaf of each individual
323 (Fig. 2e). All lines in the stress treatment presented a significant reduction in stomatal conductance during
324 moderate stress (HDG11-2 $p < 0.01$; WT $p < 0.001$) and severe stress (HDG11-2 $p < 0.05$; WT $p < 0.01$). During
325 moderate stress, stressed WT plants presented stomatal conductance values ranging from 96 to 366 mmol m^{-2}

326 s^{-1}, which, although not significant, differed from those of HDG11-2, which ranged from 125–480 mmol m^{-2} s^{-1}.
327 During severe stress, the stomatal conductance further decreased to a range of values between 36–50 mmol m^{-}
328 ^{2} s^{-1} in the WT and 23–140 mmol m^{-2} s^{-1} in HDG11-2, with the transgenic line displaying a broader range of
329 stomatal conductance than the WT. Interestingly, although the control plants were steadily watered, a reduction
330 in leaf stomatal conductance could also be observed in the same trend as the stressed plants, although not as
331 intense. In the control treatment, a significant difference between WT and HDG11-2 was observed under
332 moderate stress ($p < 0.01$). Upon recovery, the previously stressed HDG11-2 plants presented significantly
333 greater stomatal conductance than the control plants did ($p < 0.01$), indicative of a compensatory response that
334 surpassed the stress-free state of the plants.

335 The chlorophyll content was measured on each sampling day in the 3rd fully expanded leaf of all individuals
336 (Fig. 2f). Compared with that in the control treatment, the chlorophyll content in each line significantly increased
337 in the stress treatment group ($p < 0.001$). Within each treatment group, only the control plants presented
338 significant differences. Compared with the overexpression line, the WT plants presented a highly significant
339 decrease in chlorophyll content during severe stress ($p < 0.01$).

340 As evident from the data presented in Fig. 2a–f, the drought stress treatment had a pronounced effect on both
341 lines of the stress group. Phenotypic examinations revealed notable differences between the stressed individuals
342 of WT and HDG11-2 (Fig. 2g). Under severe stress, leaf withering was observed in all stressed individuals,
343 indicating a loss of turgor. However, the leaves of the WT plants appeared more severely affected by drought,
344 resulting in a greater degree of water loss, whereas the leaves of the HDG11-2 plants remained vital, albeit
345 drooping. This observation was further supported by the conditions of the shoot tips, where all HDG11-2 plants
346 maintained vital shoot tips, in contrast to WT plants, which presented hanging and turgor loss-affected shoot tips
347 on three individuals. During the recovery phase, the shoot tips of the WT plants were unable to be restored, and
348 all individuals presented severe leaf loss. In strong contrast, all HDG11-2 individuals recovered from the drought
349 stress and presented a vital phenotype, underscoring their increased resilience to drought stress.

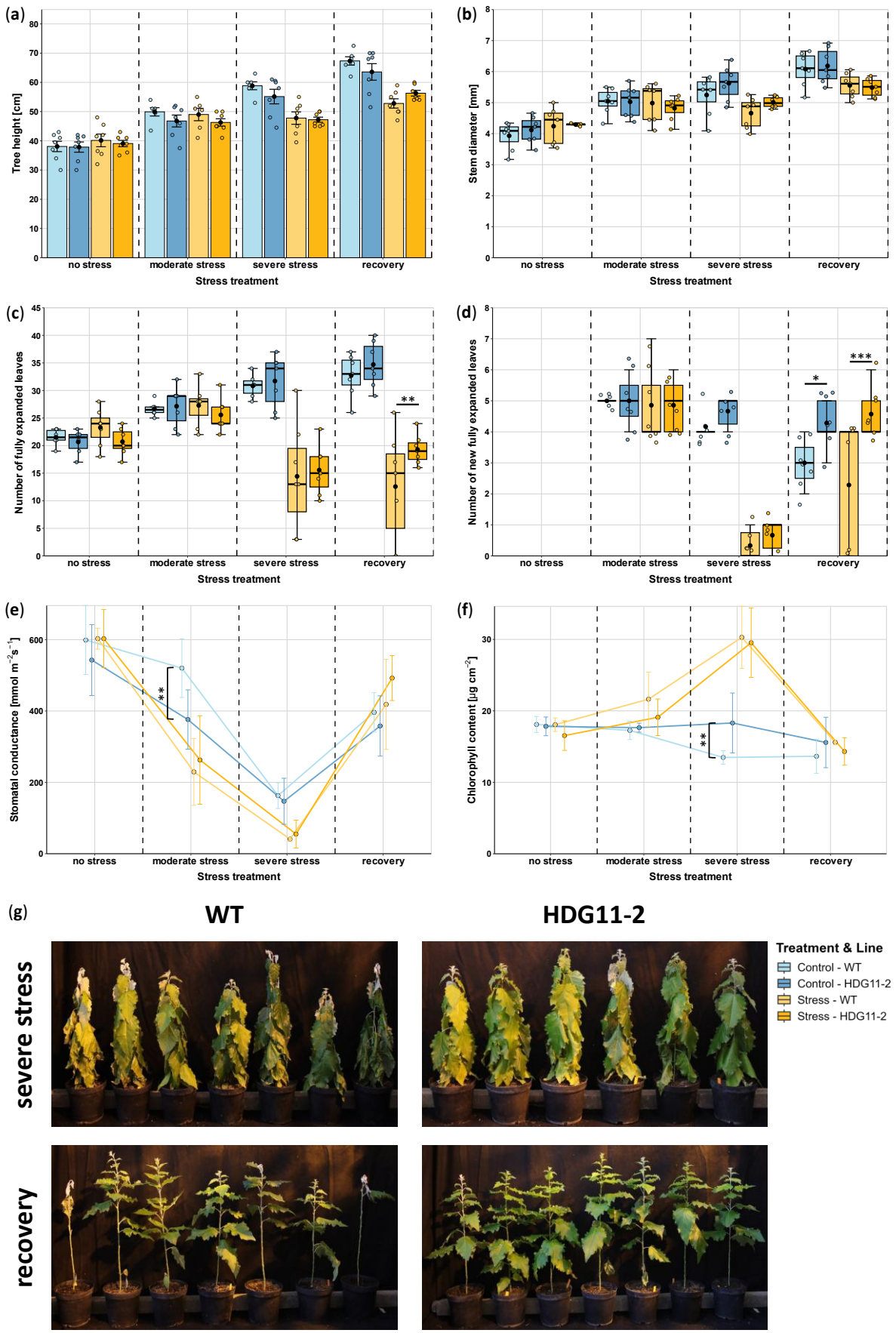
(a)
Tree height [cm]
no stress
moderate stress
severe stress
recovery
Stress treatment
(b)
Stem diameter [mm]
(c)
Number of fully expanded leaves
**
(d)
Number of new fully expanded leaves
*
***
(e)
Stomatal conductance [mmol m-2 s-1]
**
(f)
Chlorophyll content [µg cm-2]
**
(g)
WT
HDG11-2
severe stress
recovery
Treatment & Line
Control - WT
Control - HDG11-2
Stress - WT
Stress - HDG11-2

350

351 **Fig. 2** Morphological and physiological responses of WT and HDG11-2 plants under drought stress
352 conditions in the greenhouse. Measurements of (a) tree height, (b) stem diameter, (c) number
353 of fully expanded leaves, (d) number of new fully expanded leaves, (e) stomatal conductance
354 and (f) chlorophyll content. (g) Response to 14 days without water (severe stress) and
355 subsequent 7 days of rewatering (recovery). The graphs present the means ± SEs (n = 7).
356 Asterisks indicate significant differences between lines of the same treatment on the basis of
357 linear mixed-effects models with Holm-adjusted post hoc contrasts (* $p < 0.05$, ** $p < 0.01$, ***
358 $p < 0.001$). Statistically significant differences between treatments are not graphically
359 represented

360

361 The RWC of the 3rd fully expanded leaf of each individual remained consistently above 80% for both control lines
362 throughout the experiment (Fig. 3a). A significant difference in RWC was observed between the WT and HDG11-
363 2 lines in the stress group during severe stress ($p < 0.05$). In general, the RWC of both stress groups decreased
364 under severe stress, with 68% in the WT and 76% in the HDG11-2. During recovery, the RWC increased again in
365 both lines, and the significant difference in RWC between the WT and HDG11-2 plants in the stress group was
366 still consistent ($p < 0.01$). Additionally, HDG11-2 reached a level of 96%, surpassing the RWC level of the control
367 group (88%).

368 Changes at the molecular level were observed by measuring the accumulation of the stress-triggered molecules
369 proline and MDA during the experiment under the two treatments and in the two different lines. Proline and
370 MDA contents were measured on the first sampling day (no stress) as well as during severe stress and recovery.
371 The basal proline concentration ranged from 0.1 to 0.35 µmol g^{-1} FW for both lines in both treatments at the
372 beginning of the experiment (Fig. 3b). These concentrations remained relatively stable throughout the
373 experiment, with the exception of the WT line in the stress treatment. During severe stress, proline
374 concentrations increased significantly in the WT line, reaching a mean concentration of 0.61 µmol g^{-1} FW, which
375 was highly significantly different from that in the HDG11-2 overexpression line ($p < 0.001$). Although the proline
376 concentration of the WT decreased during recovery, the difference from that of HDG11-2 was still significant (p
377 < 0.01). Initially, all the lines presented low MDA accumulation (< 5 nmol g^{-1} FW) in both treatment groups, which
378 remained stable in the control groups throughout the experiment (Fig. 3c). Under severe stress, the MDA
379 concentrations increased slightly in both stressed lines, with significant differences compared with their
380 respective controls (HDG11-2 $p < 0.01$; WT $p < 0.001$). Notably, the stress group of the WT line presented a strong
381 increase in MDA concentration during recovery, with a mean value of 9.04 nmol g^{-1} FW, which was highly
382 significantly different from that of the overexpression line HDG11-2 (2.89 nmol g^{-1} FW, $p < 0.001$) and its own
383 control group (1.18 nmol g^{-1} FW, $p < 0.001$).

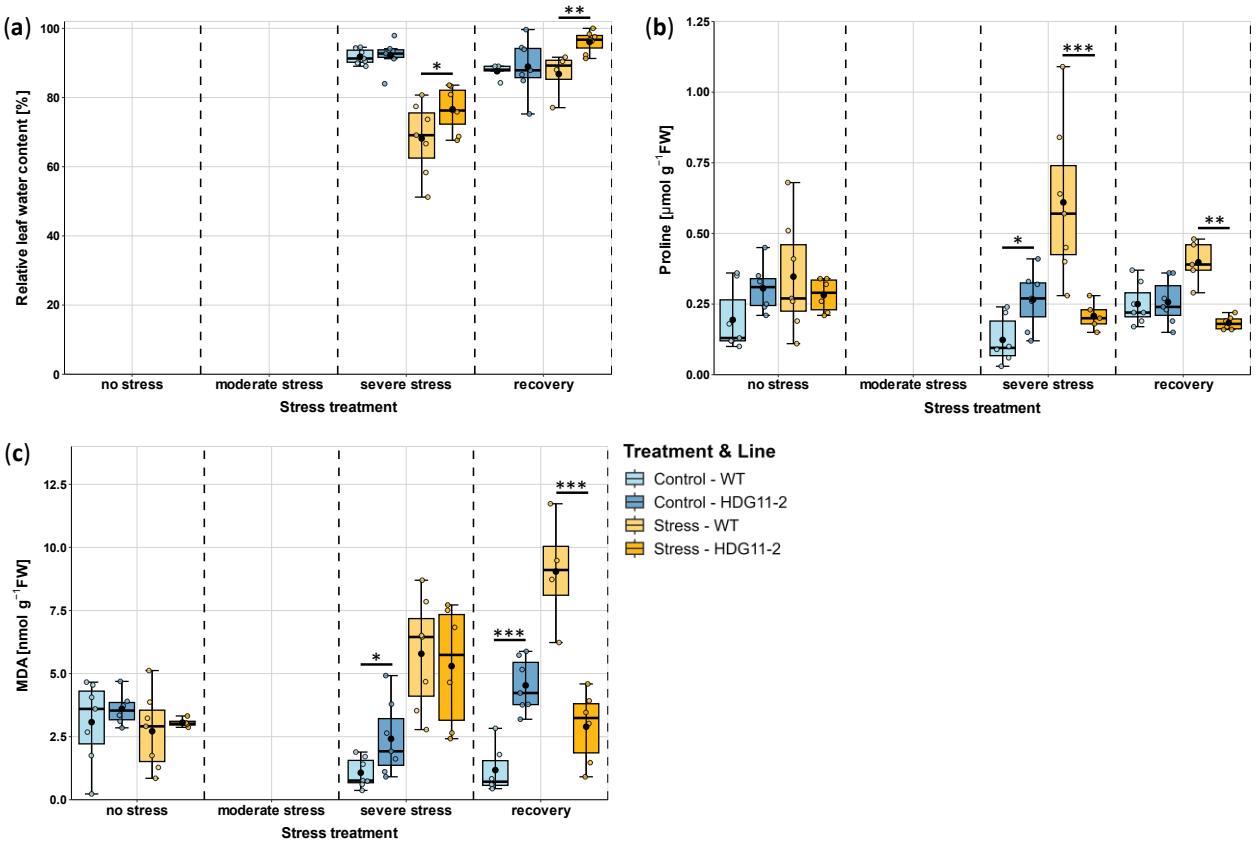

Fig. 3 Molecular physiological responses of WT and HDG11-2 plants under drought stress conditions in the greenhouse. Measurement of (a) RWC, (b) proline content, and (c) MDA content. The graphs present the means ± SEs (n = 7). Asterisks indicate significant differences between lines of the same treatment on the basis of linear mixed-effects models with Holm-adjusted post hoc contrasts (* $p < 0.05$, ** $p < 0.01$, *** $p < 0.001$). Statistically significant differences between treatments are not graphically represented

Trichome phenotyping

During the first experiment in the greenhouse, we observed that the individuals of the HDG11-2 line presented a glabrous phenotype characterized by a lack of trichomes on both the abaxial leaf side and the stem. This phenotype was also observed in *in vitro*-grown plantlets of the HDG11-2 line. Light microscopic examination confirmed the complete loss of trichomes in these individuals, whereas WT individuals presented typical trichome density (Fig. 4).

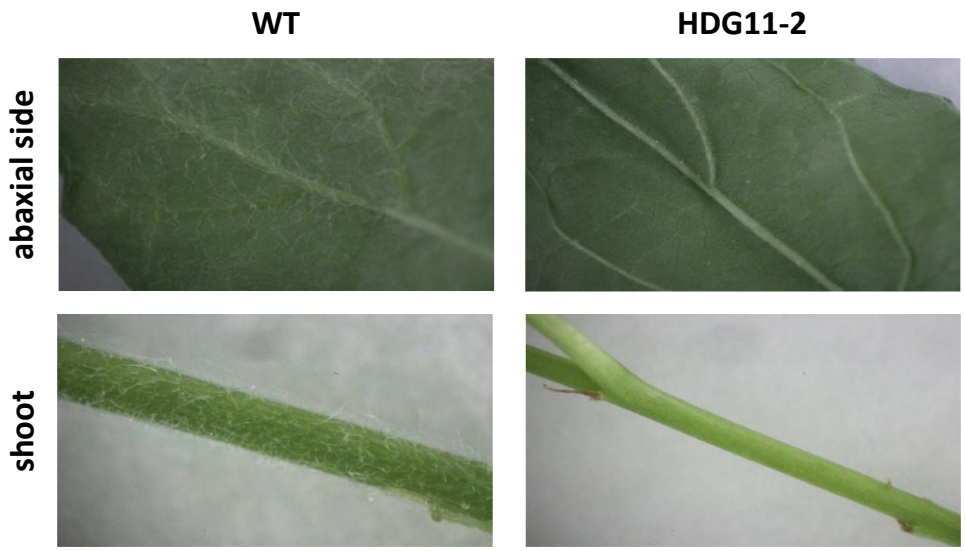

Fig. 4 Microscopic examination of the abaxial leaf surface and stem of *in vitro*-grown WT and HDG11-2 plants. HDG11-2 was notable for its glabrous phenotype

Gene expression analyses

The expression of the candidate gene *PtaHDG11* and the downstream genes *PtaSOD2-like* and *PtaCAT2-like*, both of which have antioxidative functions, as well as *PtaSDD1*, which is involved in stomatal density and distribution, was analyzed. The relative expression, expressed as the fold change compared with that of the WT controls under both treatments, revealed significantly greater expression of the candidate gene *PtaHDG11* in the HDG11-2 transgenic line during severe stress ($p < 0.05$) (Fig. 5a). Although not significant, the transgenic line also presented approximately doubled gene expression in the control treatment. Given the enhanced drought stress tolerance of the overexpression lines in the greenhouse experiment, we were interested in the gene expression of antioxidant genes. HDG11-2 presented nearly fourfold greater expression of *PtaSOD2-like* than did the WT under severe stress ($p < 0.05$, Fig. 5b). Similar results were obtained for *PtaCAT2-like*, where line HDG11-2 displayed almost 2.5-fold higher, highly significant gene expression under severe stress ($p < 0.01$, Fig. 5c). Overall, the gene expression analyses of the antioxidant genes *PtaSOD2* and *PtaCAT2* revealed significant upregulation in HDG11-2, mainly under stress conditions. The expression of *PtaSDD1* was highly significantly downregulated in the overexpression line under severe stress ($p < 0.01$, Fig. 5d). The involvement of the *PtaSDD1* gene in regulating stomatal leaf density suggests that its downregulation in the transgenic line might be associated with reduced stomatal density. However, a subsequent microscopic analysis of the stomatal density in *in vitro*-grown WT and HDG11-2 plants revealed no significant difference between the two lines, although HDG11-2 appeared to have a slightly lower stomatal density (Online Resource 4). Gene expression analysis of *PtaGL2*, a gene positively associated with trichome development, revealed significant upregulation in HDG11-2 under controlled conditions in the greenhouse, providing insight into the disturbed genetic regulation of trichome formation (Online Resource 5). In addition, the *PtaXTH32-like* gene, which is a xyloglucan endotransglycosylase/hydrolase

422 that is involved in cell wall plasticity and extensibility, was highly significantly upregulated in the line HDG11-2
423 under both treatments (Fig. 5e).

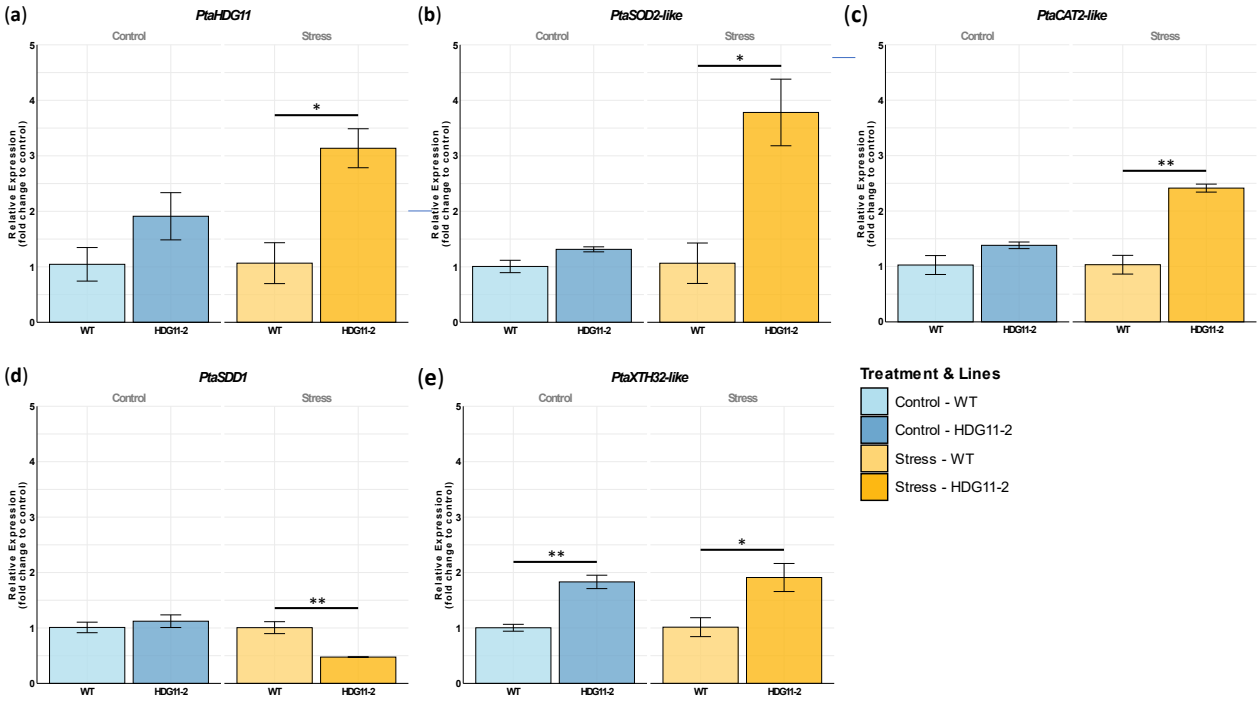

424

425 **Fig. 5** Gene expression analyses of WT and HDG11-2 in response to severe drought stress in a
426 greenhouse experiment. Expression analyses of (a) *PtaHDG11*, (b) *PtaSOD2-like*, (c) *PtaCAT2-*
427 *like*, (d) *PtaSDD1* and (e) *PtaXTH32-like*. The graphs present the means ± SEs (n = 3). Asterisks
428 indicate significant differences between lines within the same treatment, based on Student's t
429 test (* $p < 0.05$, ** $p < 0.01$)

430 **Climate chamber stress experiment**

431 To further test and validate the increased drought stress tolerance observed in the greenhouse experiment, a
432 climate chamber drought stress experiment was conducted on lines HDG11-2 and WT, with a higher number of
433 individuals per treatment. Similar to the first experiment, no significant differences in tree height were observed
434 between WT and HDG11-2 under the same treatment conditions (Fig. 6a). The height of the control plants in
435 both lines steadily increased, with an average increase of approximately 12 cm over the course of the
436 experiment. In contrast, during severe stress, plants of both lines subjected to drought stress presented cessation
437 of growth, resulting in significant differences compared with their respective control lines (WT $p < 0.05$; HDG11-
438 2 $p < 0.001$), which persisted during the recovery phase ($p < 0.01$). However, both lines in the stress group
439 resumed growth during the recovery period, ultimately achieving a mean height increase of approximately
440 10 cm. Similar results were observed for stem diameter, although significant differences were noted between
441 HDG11-2 and the stress group of WT during recovery, with HDG11-2 exhibiting a thicker stem ($p < 0.05$, Fig. 6b).
442 Overall, the HDG11-2 line initially presented a greater stem diameter and tree height than the WT line did (albeit

443 not significantly), ultimately surpassing the WT line in terms of these growth parameters by the end of the
444 experiment.

445 A pronounced phenotypic difference emerged between WT and HDG11-2 within the stress treatment group (Fig.
446 6c). The number of fully expanded leaves highly significantly differed between the two lines during severe stress
447 and the following recovery phase. On average, HDG11-2 presented 7 more leaves per individual ($p < 0.001$).
448 Significant differences in the number of fully expanded leaves within the same line and between the two
449 treatments were no longer apparent in HDG11-2 during recovery, underscoring the robust recovery of growth
450 parameters in the HDG11-2 overexpression line. This result is further supported by the examination of newly
451 developed leaves (Fig. 6d). Compared with WT plants, HDG11-2 plants presented significantly more new leaves
452 in the stress group during severe stress ($p < 0.001$). Additionally, HDG11-2 was not significantly different between
453 the two treatments during severe stress, in contrast to the WT ($p < 0.001$).

454 The stomatal conductance followed the trends observed during the greenhouse experiment. Severe drought
455 stress led to a reduction in stomatal conductance in both stressed lines, with mean values of 72 mmol m^{-2} s^{-1} in
456 WT and 95 mmol m^{-2} s^{-1} in HDG11-2 (Fig. 6e). During the recovery phase (Fig. 6f), stomatal conductance increased
457 again in both stressed lines, with HDG11-2 exhibiting a significant increase that surpassed that of the control
458 group ($p < 0.05$). Although less pronounced than that in the greenhouse experiment, the stomatal conductance
459 also decreased in the control treatment lines throughout the experiment.

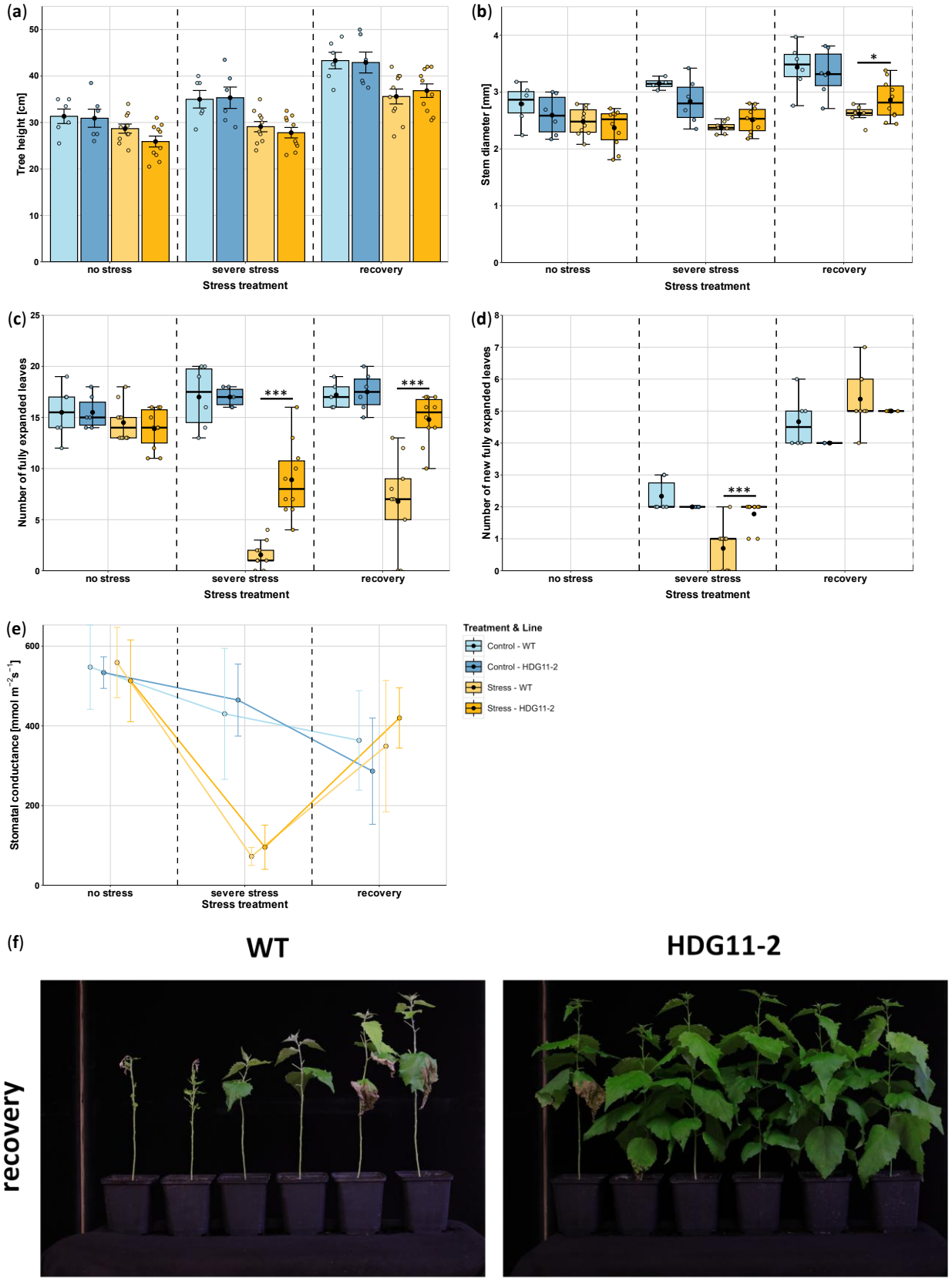

Fig. 6 Morphological and physiological responses of WT and HDG11-2 plants under drought stress conditions in a climate chamber. Measurements of (a) tree height, (b) stem diameter, (c) number

463 of fully expanded leaves, (d) number of new fully expanded leaves, and (e) stomatal
464 conductance. (f) Mean six individuals of WT and HDG11-2 after 14 days of rewatering (recovery)
465 following the stress period. The graphs present the means ± SEs (control treatment, n = 6; stress
466 treatment, n = 10). Asterisks indicate significant differences between lines of the same
467 treatment on the basis of linear mixed-effects models with Holm-adjusted post hoc contrasts (*
468 $p < 0.05$, ** $p < 0.01$, *** $p < 0.001$). Statistically significant differences between treatments are
469 not graphically represented

470

471 To gain insight into the water content and available water in the plants' leaves, the RWC was measured in the 3rd
472 fully expanded leaf of each individual (Fig. 7a). A significant difference in RWC was observed between the WT
473 and HDG11-2 lines within the stress treatment during the severe stress. Compared with the WT line, the
474 overexpression line presented, on average, a 17% greater RWC ($p < 0.001$). Additionally, VWC measurements of
475 the soil moisture revealed a significantly higher VWC in the stressed HDG11-2 line (Online Resource 6).

476 The mean proline concentration was low, around 0.11 µmol g^{-1} FW, for all the lines and treatments on all the
477 sampling days, except for the stress-treated WT during severe stress (Fig. 7b). Here, the proline concentration
478 increased to a mean value of 0.78 µmol g^{-1} FW, resulting in a highly significant difference compared with that of
479 the stressed HDG11-2 line ($p < 0.001$). Notably, the proline concentration decreased during the recovery phase,
480 returning to a relatively low level. In contrast, a significant difference in the MDA concentration was observed
481 between the WT line and HDG11-2 ($p < 0.05$, Fig. 7c).

482 After 14 days of recovery, the aboveground biomass of all the plants was harvested, oven-dried, and weighed
483 (Fig. 7d). The results revealed that the HDG11-2 overexpression line presented significantly greater dry shoot
484 biomass ($p < 0.01$), which was consistent with the morphological parameters measured earlier. These findings
485 further support the enhanced drought stress tolerance of the HDG11 overexpression line.

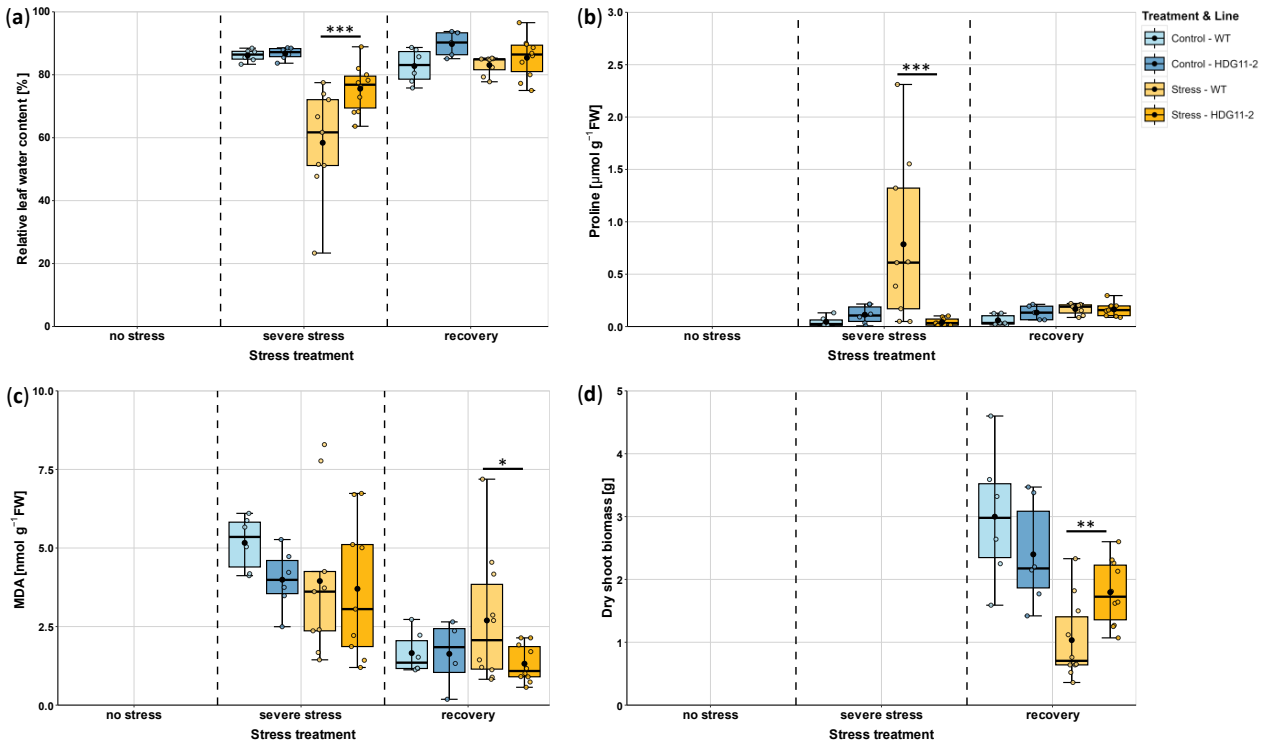

Fig. 7 Molecular physiological and physiological responses of WT and HDG11-2 plants under drought stress conditions inside a climate chamber. Measurements of (a) RWC, (b) proline content, (c) MDA content, and (d) dry shoot biomass. The graphs present the means ± SEs (control treatment, n = 6; stress treatment, n = 10). Asterisks indicate significant differences between lines of the same treatment on the basis of linear mixed-effects models with Holm-adjusted post hoc contrasts (* $p < 0.05$, ** $p < 0.01$, *** $p < 0.001$). Statistically significant differences between treatments are not graphically represented

A significant positive correlation was observed between the RWC and VWC under severe drought stress in the HDG11-2 line of the stress group (Spearman's $\rho = 0.95$, $p < 0.001$; Fig. 8a). Plants with higher soil moisture contents consistently showed higher internal water contents. In contrast, the RWC and VWC of the WT line were not significantly correlated (Spearman's $\rho = -0.1$, $p = 0.81$). The data revealed distinct clustering by genotype, with the WT plants showing a distribution over the lower range of VWC values (spanning from < 1% to 7%) and the HDG11-2 line primarily distributed within a higher VWC range (spanning almost exclusively from 3% to 15%). Furthermore, at comparable VWC levels, the HDG11-2 line consistently maintained a higher RWC than did the WT.

Additionally, a significant positive correlation was detected between RWC and stomatal conductance under severe drought stress in the HDG11-2 line (Fig. 8b). The HDG11-2 line presented a positive correlation with Spearman's $\rho = 0.76$ ($p < 0.05$), maintaining a greater RWC and stomatal conductance than those of the WT under

506 the same stress conditions. The data points for the HDG11-2 line were clustered in the right quadrants of the
507 plot, indicating a more linear adaptation to changes in RWC, whereas the WT data points were located almost
508 horizontally over the whole RWC range.

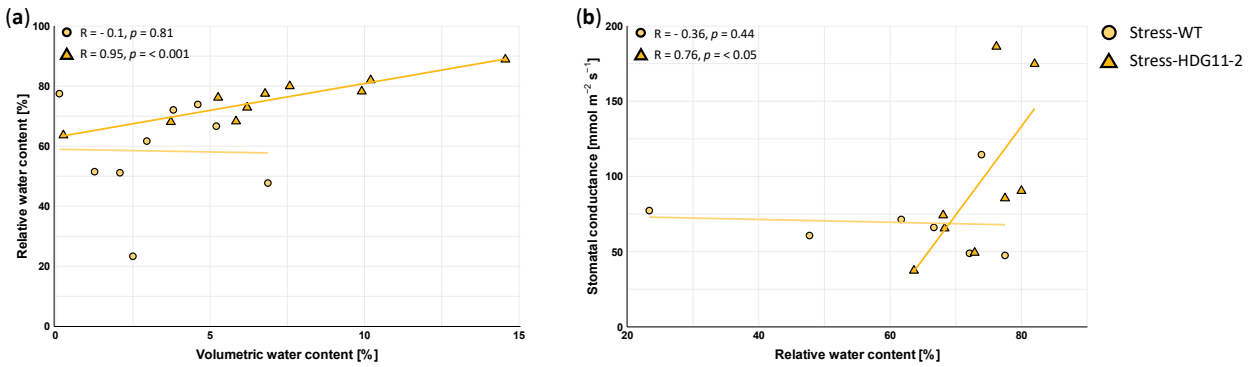

509

510 **Fig. 8** Spearman correlations between the WT and HDG11-2 lines under severe stress in the climate
511 chamber experiment. (a) VWC and RWC were significantly positively correlated in the HDG11-2
512 line, indicating a more stable water status. (b) The correlation between RWC and stomatal
513 conductance also showed a significant positive correlation in the HDG11-2 line, suggesting
514 coordinated regulation of water balance and gas exchange in HDG11-2. Significant differences
515 between lines are based on Student's t-test. n = 10

516 ## Discussion

517 In two independent drought stress experiments, we demonstrated increased drought stress tolerance in a
518 transgenic *P. tremula* × *P. alba* line constitutively overexpressing the *PtaHDG11* gene. Comprehensive
519 phenotyping, which encompasses morphological, physiological, molecular physiological, and genetic aspects,
520 revealed several parameters associated with improved drought stress tolerance in the genetically modified
521 poplars.

522 **Morphology and growth**

523 From a morphological perspective, plants with smaller stature and reduced leaf area, either by fewer or smaller
524 leaves, tend to have enhanced drought stress tolerance because of their ability to limit water loss and maintain
525 essential physiological functions (Toscano et al. 2019). In our experiment, only minimal differences between the
526 overexpression line and the WT were observed during the stress experiments in terms of height and stem growth.
527 All plant lines exhibited similar growth rates under control conditions, with no significant differences. Only the
528 stressed HDG11-2 line presented a thicker stem after recovery in the climate chamber experiment. Therefore,
529 the observed drought stress tolerance of the *HDG11*-overexpressing poplars clearly did not arise from reduced
530 growth.

531 In response to drought, poplars undergo leaf abscission to reduce transpiration and, consequently, water loss
532 when a critical threshold is exceeded. This adaptive response comes at the cost of reduced leaf area, which in
533 turn impairs photosynthetic productivity, highlighting the trade-off between drought tolerance and carbon
534 assimilation in poplars (Larchevêque et al. 2011). Across all the experiments, we consistently observed a
535 significantly greater rate of leaf abscission in the WT poplars, which was concomitant with a substantial reduction
536 in biomass production at the end of the climate chamber experiment.

537 During the 21-day greenhouse experiment, the WT controls produced fewer new leaves than they did at the
538 beginning, whereas HDG11-2 maintained a constant leaf-emergence rate under control conditions. The reduced
539 leaf production in the control WT plants over the time of the greenhouse experiment suggests an age-related or
540 nutrient-related decline. HD-ZIP IV factors are known to regulate epidermal differentiation and meristem activity
541 (Tu et al. 2022). Therefore, *PtaHDG11* may sustain shoot-apical meristem competence, delaying age- or nutrient-
542 induced decline in HDG11-2. The lack of a similar effect in the climate chamber experiment may be due to its
543 shorter duration, which may not have been sufficient to induce nutrient deficiency or age-related effects.

544 **Water retention and cell wall remodeling**

545 Although all the plants were treated equally, HDG11-2 was able to maintain higher RWC in its leaves, potentially
546 reducing stress and preventing the dehydration threshold that triggers abscission. A possible explanation for this
547 phenomenon lies in the observed higher expression of the *PtaXTH32-like* gene. *XTH* genes are involved in cell
548 wall plasticity and extensibility (Le Gall et al. 2015). Previous studies have shown that plants with altered cell wall
549 elasticity contribute to the maintenance of cell turgor, which subsequently increases drought stress tolerance
550 (Martínez et al. 2007; Coutinho et al. 2021). The overexpression of *PagXTH12* in poplar also increased drought
551 stress tolerance, likely by enhancing the regulation of cell wall modifications (Yuan et al. 2024). Moreover, many
552 cell wall loosening proteins, including *AtXTH32*, possess HD-ZIP cis-elements in their promoters that can be bound
553 by *AtHDG11*, allowing it to potentially regulate their expression. We therefore propose that increased *XTH*
554 activity contributes to the maintenance of turgor and higher RWC, although this hypothesis should be further
555 tested by direct wall mechanics assays such as extensometry.

556 **Stomatal regulation and photosynthetic acclimation**

557 Decreasing soil moisture negatively impacts the water status of many plants, as evidenced by a reduction in RWC
558 and a decrease in stomatal conductance, which is an adaptive mechanism to conserve water and minimize water
559 loss (Xiong et al. 2022; Pinto et al. 2023). In our experiments, all the stressed lines presented reduced stomatal
560 conductance under drought stress. Under severe drought in the climate chamber, HDG11-2 displayed a wide
561 distribution of stomatal conductance that was positively correlated with RWC, whereas the WT maintained flat
562 stomatal conductance regardless of leaf water status, implying a loss of regulation and stress-induced stomatal
563 shutdown. Concomitantly, *PtaSDD1* was strongly downregulated in HDG11-2. *SDD1* encodes a negative regulator

564 of the stomatal lineage (Xia et al. 2024). Although stomatal density analyses of *in vitro* seedlings revealed a
565 non-significant trend toward fewer stomata in HDG11-2, the direction matches the transcriptional repression
566 measured during drought stress in the greenhouse and parallels findings in triploid poplar, where reduced
567 stomatal density lowered transpiration and stabilized RWC (Li et al. 2021).

568 Under severe drought, all the plants presented increased chlorophyll in the upper canopy. A similar response has
569 been reported for other poplars, especially those under mild water deficit (Tian et al. 2024). The increased
570 accumulation of chlorophyll in the upper leaf layer may serve to improve light energy absorption or may be a
571 result of carbon redistribution from older to younger leaves to promote photosynthesis (Yao et al. 2024). The
572 response is therefore a general drought acclimation trait rather than a line-specific effect.

573 **Molecular stress markers—proline, MDA, and antioxidant gene expression**

574 To gain further insight into the molecular stress response, proline levels, which are known to increase under
575 water stress, were measured. The proline levels did not increase significantly in the *HDG11* overexpression line,
576 whereas they did in the WT plants. The overexpression line did not significantly differ from the basal proline
577 concentrations of the control lines at any stress time point. Interestingly, this observation differs from the results
578 in *A. thaliana*, *F. arundinacea*, *O. sativa*, *B. oleracea,* and *G. hirsutum,* where the overexpression of *AtHDG11* at
579 all times leads to increased proline accumulation under stress and in some cases even under control conditions
580 (Yu et al. 2008; Cao et al. 2009; Yu et al. 2013; Yu et al. 2016; Zhu et al. 2016). These results suggest that the
581 *PtaHDG11* overexpression line may not have experienced significant oxidative stress. This notion is supported by
582 the relatively low levels of MDA, a commonly used indirect marker for oxidative stress, measured in HDG11-2.
583 Notably, although the MDA levels increased under severe stress conditions in the greenhouse experiment, they
584 rapidly returned to baseline levels after the recovery period. In contrast, the WT plants continued to accumulate
585 MDA during recovery in both experiments, suggesting lingering lipid peroxidation due to inefficient ROS
586 detoxification. This observation implies that HDG11-2 plants may not require proline accumulation, as the cellular
587 stress response appears to be tightly regulated. The transient increase in MDA levels under severe stress
588 conditions may reflect a concomitant rise in ROS, and emerging evidence suggests that MDA itself can act as a
589 signaling molecule to regulate stress responses (Morales and Munné-Bosch 2019). The higher observed RWC and
590 increased leaf numbers in HDG11-2 suggest greater energy availability for ROS detoxification, enabling better
591 management of oxidative stress and maintaining cellular homeostasis under severe stress conditions (Choudhury
592 et al. 2017). In line with these findings, our gene expression analyses of the antioxidant genes *SOD2-like* and
593 *CAT2-like* revealed significantly greater expression in HDG11-2 under stress conditions in the greenhouse. The
594 interplay of these antioxidant genes may increase the production of antioxidants and support the degradation
595 of harmful ROS.

596 **Trichome loss in HDG11-2**

597 In addition to enhanced drought tolerance, a unique phenotype characterized by the complete absence of
598 trichomes was observed in HDG11-2. This complete suppression of trichome formation is consistent with the
599 established role of the HD-ZIP IV transcription factor *AtHDG11* as a negative regulator of trichome differentiation,
600 in contrast with the positive regulatory function of the homologous HD-ZIP IV TF *AtGL2* (Rerie et al. 1994;
601 Nakamura et al. 2006; Lin and Aoyama 2012; Ahmad et al. 2024). This potent phenotypic effect was highly
602 stringent. In this phenotypically affected line, we observed a significant upregulation of *PtaGL2* expression under
603 well-watered conditions, which is likely a direct transcriptional consequence of *PtaHDG11* overexpression.
604 Despite this induction, trichome formation remained completely suppressed, indicating that the developmental
605 block imposed by the overexpression is too strong to be complemented by *PtaGL2* expression. The *HDG11* gene
606 belongs to a TF family deeply embedded in plant development, where the HD-ZIP IV subfamily is known for its
607 pleiotropic involvement in various processes, including epidermal cell differentiation, root development, and
608 meristem activity (Horstman et al. 2015; Qiu et al. 2022). Recent studies have provided more insight into the role
609 of HD-ZIP IV TFs in trichome development in various plant species (Cui et al. 2025; Li et al. 2025; Zocca et al.
610 2025). Our findings confirm that *PtaHDG11* acts within this broader developmental framework by influencing cell
611 differentiation (trichome suppression), although its detailed regulatory network in poplar with respect to
612 trichome development requires further investigation.

613 Furthermore, the observation that the *PtaHDG11* transgene significantly enhances drought stress tolerance in
614 the transgenic line adds a crucial stress-related dimension. HDG11-2 surpassed the drought stress tolerance of
615 the WT, despite the morphological difference in trichome formation. Trichomes are epidermal structures on
616 plant leaves and shoots that serve as a barrier against pathogens or UV protection (Fambrini and Pugliesi 2019).
617 Leaf trichomes have also been found to be involved in foliar water uptake, e.g., as described for the deciduous
618 tree species *Fagus sylvatica* (Schreel et al. 2020; Li et al. 2023). To our knowledge, water uptake through
619 trichomes has not been explored in poplars. Because trichome-less HDG11-2 maintained a greater RWC and
620 fewer drought stress symptoms than did the trichome-bearing WT under identical humidity, we hypothesize that
621 foliar water uptake via trichomes does not contribute to drought tolerance in this hybrid.

622 **Conserved HD-ZIP IV function and a species-specific proline response**

623 The suite of stress-related responses observed in the *PtaHDG11* transgenic poplars mirrored the patterns
624 reported for *AtHDG11* overexpression in herbaceous species, underscoring the conserved role of this HD-ZIP IV
625 transcription factor in conferring drought resilience. Sequence alignment confirmed that the two proteins share
626 approx. 68% overall identity, with > 95% and > 89% identity of the homeodomain and START domain,
627 respectively, that mediate DNA binding and co-factor interaction (Wang et al. 2013). Despite this high degree of
628 similarity, a striking divergence emerges in proline metabolism, where in the poplar background, proline
629 accumulates only in the stressed WT, whereas *AtHDG11* overexpression in most herbaceous systems triggers a

630 pronounced proline surge. This discrepancy points to a species-specific downstream wiring of the *HDG11*
631 regulatory network rather than to differences in the transcription factor itself.

632 **Implications for breeding and forest-ecosystem resilience**

633 The pronounced improvements in leaf water retention, oxidative protection, and shoot biomass identify
634 *PtaHDG11* as a promising target for enhancing drought resilience in forest trees. The use of its native promoter
635 can be incorporated into marker-assisted selection pipelines to accelerate the development of tolerant cultivars
636 for short-rotation coppice and timber production, where water stress can severely curtail biomass yields. The
637 results of the present study should also be extrapolated to other tree species, allowing for the examination of
638 genetic and genomic variation in *HDG11* and its regulatory elements in different tree species. These findings can
639 facilitate the identification of new breeding partners and the development of effective breeding strategies to
640 increase drought stress tolerance in trees. The insights into *HDG11* can guide the selection of drought-tolerant
641 tree genotypes, thereby supporting the development of more resilient and adaptable forest ecosystems.

642 Acknowledgments

643 We are grateful to Susanne Jelkmann for excellent technical assistance, as well as Alice-Jeannine Sievers, Katrin
644 Groppe, and Vivian Kuhlenkamp for the support within the greenhouse experiment. We thank Sabrina Maninger,
645 Wolfgang Graf, as well as Sabine Benischek and Monika Spauszus for the installation of the drip irrigation system
646 and plant cultivation, respectively. This work was funded by the German Federal Ministry of Food and Agriculture
647 through the funding agency Fachagentur Nachwachsende Rohstoffe (project "TreeEdit", grant no. 2219NR359).
648 Open Access funding enabled and organized by Project DEAL.

649 Competing interests

650 The authors declare no competing interests.

651 Authors' Contributions

652 AF, MF, and TB designed the research. AF performed the research and analyzed the data. AF and TB interpreted
653 the data. AF and TB wrote the manuscript, and all the authors edited the text. MF and TB received the funding.

654 Data Availability Statement

655 The data of this study are available at the corresponding author upon reasonable request.

656 ## Supplementary Information

657 Online Resource 1: Transformation vector

658 Online Resource 2: Primers used for molecular analyses

659 Online Resource 3: Volumetric water content in the greenhouse experiment

660 Online Resource 4: Analysis of stomatal density in WT and HDG11-2 poplars

661 Online Resource 5: Expression of *PtaGL2* in WT and HDG11-2 poplars under control and stress conditions

662 Online Resource 6: Volumetric water content in the climate chamber experiment under severe stress conditions

663 ## References

664 Abrahám E, Hourton-Cabassa C, Erdei L, Szabados L (2010) Methods for determination of proline in plants.
665 Methods Mol Biol 639:317–331

666 Ahmad B, Lerma-Reyes R, Mukherjee T, Nguyen HV, Weber AL, Cummings EE, Schulze WX, Comer JR, Schrick K
667 (2024) Nuclear localization of Arabidopsis HD-Zip IV transcription factor GLABRA2 is driven by importin α. J Exp
668 Bot 75:6441–6461

669 An Y, Liu Y, Liu Y, Lu M, Kang X, Mansfield SD, Zeng W, Zhang J (2021) Opportunities and barriers for biofuel and
670 bioenergy production from poplar. GCB Bioenergy 13:905–913

671 Apel K, Hirt H (2004) Reactive oxygen species: metabolism, oxidative stress, and signal transduction. Annu Rev
672 Plant Biol 55:373–399

673 Barchet GLH, Dauwe R, Guy RD, Schroeder WR, Soolanayakanahally RY, Campbell MM, Mansfield SD (2014)
674 Investigating the drought-stress response of hybrid poplar genotypes by metabolite profiling. Tree Physiol
675 34:1203–1219

676 Bastos A, Orth R, Reichstein M, Ciais P, Viovy N, Zaehle S, Anthoni P, Arneth A, Gentine P, Joetzjer E, Lienert S,
677 Loughran T, McGuire PC, O S, Pongratz J, Sitch S (2021) Vulnerability of European ecosystems to two compound
678 dry and hot summers in 2018 and 2019. Earth Syst Dynam 12:1015–1035

679 Bates LS, Waldren RP, Teare ID (1973) Rapid determination of free proline for water-stress studies. Plant Soil
680 39:205–207

681 Bruegmann T, Fladung M, Schroeder H (2022) Flexible DNA isolation procedure for different tree species as a
682 convenient lab routine. Silvae Genetica 71:20–30

683 Bruegmann T, Orgel F, Jelkmann S, Schroeder H (2024) Isolation of high quality RNA from tree leaves using
684 Polyclar in the Spectrum Plant Total RNA Kit v1

685 Bruegmann T, Polak O, Deecke K, Nietsch J, Fladung M (2019) Poplar Transformation. Methods Mol Biol
686 1864:165–177

687 Cao Y-J, Wei Q, Liao Y, Song H-L, Li X, Xiang C-B, Kuai B-K (2009) Ectopic overexpression of *AtHDG11* in tall
688 fescue resulted in enhanced tolerance to drought and salt stress. Plant Cell Rep 28:579–588

689 Chen Y, Chen Y, Li W, Zhang H (2003) Response of the accumulation of proline in the bodies of *Populus*
690 *euphratica* to the change of groundwater level at the lower reaches of Tarim River. Chin Sci Bull 48:1995–1999

691 Choudhury FK, Rivero RM, Blumwald E, Mittler R (2017) Reactive oxygen species, abiotic stress and stress
692 combination. Plant J 90:856–867

693 Coutinho FS, Rodrigues JM, Lima LL, Mesquita RO, Carpinetti PA, Machado JPB, Vital CE, Vidigal PM, Ramos
694 MES, Maximiano MR, Mehta A, Oliveira MGA, Fontes EPB, Oliveira Ramos HJ de (2021) Remodeling of the cell
695 wall as a drought-tolerance mechanism of a soybean genotype revealed by global gene expression analysis.
696 aBIOTECH 2:14–31

697 Cui Z, Miao C, Shang H, Zhao Q, Li S, Zhang Z, Wang Y, Huang X (2025) Genome-wide identification of HD-Zip
698 transcription factor family in *Artemisia argyi* and functional analysis of *AaHDZ64* in trichome development.
699 Plant Gene 43:100529

700 Fambrini M, Pugliesi C (2019) The Dynamic Genetic-Hormonal Regulatory Network Controlling the Trichome
701 Development in Leaves. Plants (Basel, Switzerland) 8

702 Fang Y, Xiong L (2015) General mechanisms of drought response and their application in drought resistance
703 improvement in plants. Cell Mol Life Sci 72:673–689

704 Fladung M, Ahuja MR (1995) "Sandwich" method for nonradioactive hybridization. Biotechniques 18:800–802

705 Fladung M, Polak O (2012) *Ac*/Ds-transposon activation tagging in poplar: a powerful tool for gene discovery.
706 BMC Genomics 13:61

707 Goodstein DM, Shu S, Howson R, Neupane R, Hayes RD, Fazo J, Mitros T, Dirks W, Hellsten U, Putnam N,
708 Rokhsar DS (2012) Phytozome: a comparative platform for green plant genomics. Nucleic Acids Res 40:D1178-
709 86

710 Hodges DM, DeLong JM, Forney CF, Prange RK (1999) Improving the thiobarbituric acid-reactive-substances
711 assay for estimating lipid peroxidation in plant tissues containing anthocyanin and other interfering
712 compounds. Planta 207:604–611

713 Horstman A, Fukuoka H, Muino JM, Nitsch L, Guo C, Passarinho P, Sanchez-Perez G, Immink R, Angenent G,
714 Boutilier K (2015) AIL and HDG proteins act antagonistically to control cell proliferation. Development 142:454–
715 464

716 Joshi R, Wani SH, Singh B, Bohra A, Dar ZA, Lone AA, Pareek A, Singla-Pareek SL (2016) Transcription Factors
717 and Plants Response to Drought Stress: Current Understanding and Future Directions. Front Plant Sci 7:1029

718 Knutzen F, Averbeck P, Barrasso C, Bouwer LM, Gardiner B, Grünzweig JM, Hänel S, Haustein K, Johannessen
719 MR, Kollet S, Müller MM, Pietikäinen J-P, Pietras-Couffignal K, Pinto JG, Rechid D, Rousi E, Russo A, Suarez-
720 Gutierrez L, Veit S, Wendler J, Xoplaki E, Gliksman D (2025) Impacts on and damage to European forests from
721 the 2018–2022 heat and drought events. Nat Hazards Earth Syst Sci 25:77–117

722 Komán S, Németh R, Báder M (2023) An Overview of the Current Situation of European Poplar Cultures with a
723 Main Focus on Hungary. Appl Sci-Basel 13:12922

724 Landi M (2017) Commentary to: "Improving the thiobarbituric acid-reactive-substances assay for estimating
725 lipid peroxidation in plant tissues containing anthocyanin and other interfering compounds" by Hodges et al.,
726 Planta (1999) 207:604-611. Planta 245:1067

727 Larchevêque M, Maurel M, Desrochers A, Larocque GR (2011) How does drought tolerance compare between
728 two improved hybrids of balsam poplar and an unimproved native species? Tree Physiol 31:240–249

729 Le Gall H, Philippe F, Domon J-M, Gillet F, Pelloux J, Rayon C (2015) Cell Wall Metabolism in Response to Abiotic
730 Stress. Plants (Basel, Switzerland) 4:112–166

731 Leple JC, Brasileiro AC, Michel MF, Delmotte F, Jouanin L (1992) Transgenic poplars: expression of chimeric
732 genes using four different constructs. Plant Cell Rep 11:137–141

733 Letunic I, Khedkar S, Bork P (2021) SMART: recent updates, new developments and status in 2020. Nucleic
734 Acids Res 49:D458-D460

735 Leung DWM (2018) Studies of Catalase in Plants Under Abiotic Stress. In: Gupta DK, Palma JM, Corpas FJ (eds)
736 Antioxidants and Antioxidant Enzymes in Higher Plants. Springer International Publishing, Cham, pp 27–39

737 Li C, Mo Y, Wang N, Xing L, Qu Y, Chen Y, Yuan Z, Ali A, Qi J, Fernández V, Wang Y, Kopittke PM (2023) The
738 overlooked functions of trichomes: Water absorption and metal detoxication. Plant Cell Environ 46:669–687

739 Li H, Yang Y, Wang H, Liu S, Jia F, Su Y, Li S, He F, Feng C, Niu M, Wang J, Liu C, Yin W, Xia X (2021) The Receptor-
740 Like Kinase *ERECTA* Confers Improved Water Use Efficiency and Drought Tolerance to Poplar via Modulating
741 Stomatal Density. Int J Mol Sci 22

742 Li M, Fu Y, Liang X, Liu X, Huang L, Zhang S, Zhang W, Tang K, Shen Q (2025) SlHDZIV3 and SlHDZIV9 Are Two
743 Positive Regulators in the Formation of Tomato Trichomes. Plant Cell Environ 48:5789–5801

744 Lin Q, Aoyama T (2012) Pathways for epidermal cell differentiation via the homeobox gene *GLABRA2*: update
745 on the roles of the classic regulator. J Integr Plant Biol 54:729–737

746 Liu YG, Mitsukawa N, Oosumi T, Whittier RF (1995) Efficient isolation and mapping of *Arabidopsis thaliana* T-
747 DNA insert junctions by thermal asymmetric interlaced PCR. Plant J 8:457–463

748 Livak KJ, Schmittgen TD (2001) Analysis of relative gene expression data using real-time quantitative PCR and
749 the $2^{-\Delta\Delta CT}$ Method. Methods (San Diego, Calif.) 25:402–408

750 Manna M, Thakur T, Chirom O, Mandlik R, Deshmukh R, Salvi P (2021) Transcription factors as key molecular
751 target to strengthen the drought stress tolerance in plants. Physiol Plant 172:847–868

752 Martínez JP, Silva H, Ledent JF, Pinto M (2007) Effect of drought stress on the osmotic adjustment, cell wall
753 elasticity and cell volume of six cultivars of common beans (*Phaseolus vulgaris* L.). Eur J Agron 26:30–38

754 Morales M, Munné-Bosch S (2019) Malondialdehyde: Facts and Artifacts. Plant Physiol 180:1246–1250

755 Nakamura M, Katsumata H, Abe M, Yabe N, Komeda Y, Yamamoto KT, Takahashi T (2006) Characterization of
756 the class IV homeodomain-Leucine Zipper gene family in Arabidopsis. Plant Physiol 141:1363–1375

757 Pinto JR, Sloan JL, Ervan G, Burney OT (2023) Physiological and morphological responses of *Pinus ponderosa*
758 seedlings to moisture limitations in the nursery and their implications for restoration. Front Plant Sci
759 14:1127656

760 Polle A, Chen SL, Eckert C, Harfouche A (2018) Engineering Drought Resistance in Forest Trees. Front Plant Sci
761 9:1875

762 Qiu X, Wang G, Abou-Elwafa SF, Fu J, Liu Z, Zhang P, Xie X, Ku L, Ma Y, Guan X, Wei L (2022) Genome-wide
763 identification of HD-ZIP transcription factors in maize and their regulatory roles in promoting drought
764 tolerance. Physiol Mol Biol Plants 28:425–437

765 Regier N, Frey B (2010) Experimental comparison of relative RT-qPCR quantification approaches for gene
766 expression studies in poplar. BMC Mol Biol 11:57

767 Rerie WG, Feldmann KA, Marks MD (1994) The *GLABRA2* gene encodes a homeo domain protein required for
768 normal trichome development in *Arabidopsis*. Genes Dev 8:1388–1399

769 Roodbarkelari F, Groot EP (2017) Regulatory function of homeodomain-leucine zipper (HD-ZIP) family proteins
770 during embryogenesis. New Phytol 213:95–104

771 Ruan L, Chen L, Chen Y, He J, Zhang W, Gao Z, Zhang Y (2012) Expression of *Arabidopsis HOMEODOMAIN*
772 *GLABROUS 11* Enhances Tolerance to Drought Stress in Transgenic Sweet Potato Plants. J Plant Biol 55:151–158

773 Schneider CA, Rasband WS, Eliceiri KW (2012) NIH Image to ImageJ: 25 years of image analysis. Nat Methods
774 9:671–675

775 Schreel JDM, Leroux O, Goossens W, Brodersen C, Rubinstein A, Steppe K (2020) Identifying the pathways for
776 foliar water uptake in beech (*Fagus sylvatica* L.): a major role for trichomes. Plant J 103:769–780

777 Schuldt B, Buras A, Arend M, Vitasse Y, Beierkuhnlein C, Damm A, Gharun M, Grams TE, Hauck M, Hajek P,
778 Hartmann H, Hiltbrunner E, Hoch G, Holloway-Phillips M, Körner C, Larysch E, Lübbe T, Nelson DB, Rammig A,
779 Rigling A, Rose L, Ruehr NK, Schumann K, Weiser F, Werner C, Wohlgemuth T, Zang CS, Kahmen A (2020) A first
780 assessment of the impact of the extreme 2018 summer drought on Central European forests. Basic Appl Ecol
781 45:86–103

782 Tamura K, Stecher G, Kumar S (2021) MEGA11: Molecular Evolutionary Genetics Analysis Version 11. Mol Biol
783 Evol 38:3022–3027

784 Tian Q, Zhang H, Bian L, Zhou L, Ge Y (2024) Three-Dimensional Quantification and Visualization of Leaf
785 Chlorophyll Content in Poplar Saplings under Drought Using SFM-MVS. Forests 15:20

786 Toscano S, Ferrante A, Romano D (2019) Response of Mediterranean Ornamental Plants to Drought Stress.
787 Horticulturae 5:6

788 Tu Z, Yu L, Wen S, Zhai X, Li W, Li H (2022) Identification and analysis of HD-Zip genes involved in the leaf
789 development of *Liriodendron chinense* using multidimensional analysis. Plant Biol 24:874–886

790 Wang H, Li G-B, Zhang D-Y, Lin J, Sheng B-L, Han J-L, Chang Y-H (2013) Biological functions of HD-Zip
791 transcription factors. Hereditas 35:1179–1188

792 Waterhouse AM, Procter JB, Martin DMA, Clamp M, Barton GJ (2009) Jalview Version 2—a multiple sequence
793 alignment editor and analysis workbench. Bioinformatics 25:1189–1191

794 Wodtke S, Fendel A, Bruegmann T (2025) Brush them away: a simple method to remove trichomes and
795 visualize stomata. protocols.io. https://dx.doi.org/10.17504/protocols.io.kxygxwjqwv8j/v1

796 Xia Y, Han Q, Shu J, Jiang S, Kang X (2024) Stomatal density suppressor *PagSDD1* is a "generalist" gene that
797 promotes plant growth and improves water use efficiency. Int J Biol Macromol 262:129721

798 Xiong S, Wang Y, Chen Y, Gao M, Zhao Y, Wu L (2022) Effects of Drought Stress and Rehydration on
799 Physiological and Biochemical Properties of Four Oak Species in China. Plants (Basel, Switzerland) 11

800 Xu P, Cai X-T, Wang Y, Xing L, Chen Q, Xiang C-B (2014) HDG11 upregulates cell-wall-loosening protein genes to
801 promote root elongation in *Arabidopsis*. J Exp Bot 65:4285–4295

802 Yao Y, Xia L, Le Yang, Liu R, Zhang S (2024) Drought responses and carbon allocation strategies of poplar with
803 different leaf maturity. Physiol Plant 176:e14224

804 Yu H, Chen X, Hong Y-Y, Wang Y, Xu P, Ke S-D, Liu H-Y, Zhu J-K, Oliver DJ, Xiang C-B (2008) Activated expression
805 of an *Arabidopsis* HD-START protein confers drought tolerance with improved root system and reduced
806 stomatal density. Plant Cell 20:1134–1151

807 Yu L, Chen X, Wang Z, Wang S, Wang Y, Zhu Q, Li S, Xiang C (2013) Arabidopsis *Enhanced Drought*
808 *Tolerance1*/*HOMEODOMAIN GLABROUS11* confers drought tolerance in transgenic rice without yield penalty.
809 Plant Physiol 162:1378–1391

810 Yu L-H, Wu S-J, Peng Y-S, Liu R-N, Chen X, Zhao P, Xu P, Zhu J-B, Jiao G-L, Pei Y, Xiang C-B (2016) *Arabidopsis*
811 *EDT1*/*HDG11* improves drought and salt tolerance in cotton and poplar and increases cotton yield in the field.
812 Plant Biotechnol J 14:72–84

813 Yuan W, Yao F, Liu Y, Xiao H, Sun S, Jiang C, An Y, Chen N, Huang L, Lu M, Zhang J (2024) Identification of the
814 xyloglucan endotransglycosylase/hydrolase genes and the role of *PagXTH12* in drought resistance in poplar. For
815 Res 4:e039

816 Zhao Y, Lu K, Zhang W, Guo W, Chao E, Yang Q, Zhang H (2023) *PagDA1a* and *PagDA1b* expression improves
817 salt and drought resistance in transgenic poplar through regulating ion homeostasis and reactive oxygen
818 species scavenging. Plant Physiol Bioch 201:107898

819 Zhu Z, Sun B, Xu X, Chen H, Zou L, Chen G, Cao B, Chen C, Lei J (2016) Overexpression of *AtEDT1*/*HDG11* in
820 Chinese Kale (*Brassica oleracea* var. *alboglabra*) Enhances Drought and Osmotic Stress Tolerance. Front Plant
821 Sci 7:1285

822 Zocca P, van Doore E, Roovers AJM, Glas JJ, Uittenbogaard M, Verlaan MG, van Herwijnen Z, Haring MA,
823 Schuurink RC (2025) *Glandless*, a tomato HD-ZIP transcription factor, is important for the gland formation of
824 type VI trichomes. Plant J 123:e70308

825